Spin-polarized hydrogen adsorbed on the surface of superfluid 4 He

J. M. Marín, L. Vranješ Marki, and J. Boronat

Citation: The Journal of Chemical Physics **139**, 224708 (2013); doi: 10.1063/1.4843375
View online: http://dx.doi.org/10.1063/1.4843375
View Table of Contents: http://scitation.aip.org/content/aip/journal/jcp/139/22?ver=pdfcov
Published by the AIP Publishing

Spin-polarized hydrogen adsorbed on the surface of superfluid ^{4}He

J. M. Marín,[1] L. Vranješ Markić,[2] and J. Boronat[1]
[1]*Departament de Física i Enginyeria Nuclear, Universitat Politècnica de Catalunya, Campus Nord B4-B5, E-08034 Barcelona, Spain*
[2]*Faculty of Science, University of Split, HR-21000 Split, Croatia*

(Received 31 July 2013; accepted 22 November 2013; published online 13 December 2013)

The experimental realization of a thin layer of spin-polarized hydrogen H↓ adsorbed on top of the surface of superfluid ^{4}He provides one of the best examples of a stable, nearly two-dimensional (2D) quantum Bose gas. We report a theoretical study of this system using quantum Monte Carlo methods in the limit of zero temperature. Using the full Hamiltonian of the system, composed of a superfluid ^{4}He slab and the adsorbed H↓ layer, we calculate the main properties of its ground state using accurate models for the pair interatomic potentials. Comparing the results for the layer with the ones obtained for a strictly 2D setup, we analyze the departure from the 2D character when the density increases. Only when the coverage is rather small the use of a purely 2D model is justified. The condensate fraction of the layer is significantly larger than in 2D at the same surface density, being as large as 60% at the largest coverage studied. © *2013 AIP Publishing LLC*. [http://dx.doi.org/10.1063/1.4843375]

I. INTRODUCTION

Electron-spin-polarized hydrogen (H↓) was proposed a long time ago as the system in which a Bose-Einstein condensate (BEC) state could be obtained.[1,2] Intensive theoretical and experimental work was made in the 1980s and 1990s to devise experimental setups able to reach the predicted density and temperature regimes for BEC.[3–5] The high recombination rate on the walls of the containers hindered this achievement for a long time, and only after working with a wall-free confinement, Fried *et al.*[6] were able to realize its BEC in 1998. However, this was not the first BEC because three years before the BEC state was impressively obtained working with cold metastable alkali gases.[7] The same year BEC of H↓ was obtained, Safonov *et al.*[8] observed for the first time a quasi-condensate of nearly two-dimensional (2D) H↓ adsorbed on the surface of superfluid ^{4}He.

In spite of hydrogen losing the race against alkali gases to be the first BEC system, it still deserves interest for both theory and experiment. Hydrogen is the lightest and most abundant element of the Universe and, when it is spin polarized with the use of a proper magnetic field, it is the only system that remains in the gas state down to the limit of zero temperature. H↓ is therefore extremely quantum matter. A standard measure of the quantum nature of a system is the de Boer parameter[2]

$$\eta = \frac{\hbar^2}{m\epsilon\sigma^2}\,, \tag{1}$$

with ϵ and σ the well depth and core radius of the pair interaction, respectively. According to this definition, $\eta = 0.5$ for H↓ which is the largest value for η among all the quantum fluids (for instance, $\eta = 0.2$ for ^{4}He). This large value for η results from the shallow minimum (∼6 K) of the triplet potential $b\,^3\Sigma_u^+$ between spin-polarized hydrogen atoms and their small mass.[9]

Adsorption of H↓ on the surface of liquid ^{4}He has been extensively studied because of its optimal properties.[10–15] On the one hand, the interaction of any adsorbant with the ^{4}He surface is the smallest known, and on the other hand, at temperatures $T < 300$ mK the ^{4}He vapor pressure is negligible and thereby above the free surface one can reasonably assume vacuum. In fact, liquid ^{4}He was also extensively used in search of the three-dimensional (3D) H↓ BEC state when the cells were coated with helium films to avoid adsorption of H↓ on the walls and the subsequent recombination to form molecular hydrogen H_2.[3–5] Helium is chemically inert and only a small fraction of ^{3}He (6.6%) is soluble in bulk ^{4}He; spin-polarized hydrogen and its isotopes deuterium and tritium are expelled to the surface where they have a single bound state. For instance, in the case of H↓, the chemical potential of a single atom in bulk ^{4}He is[16] 36 K to be compared with the negative value on the surface, −1.14 K.[17,18,20]

The quantum degeneracy of H↓ adsorbed on ^{4}He is quantified by defining the quantum parameter $\sigma\Lambda^2$, with σ the surface density and Λ the thermal de Broglie wavelength.[15] Experiments try to increase this parameter as much as possible by increasing the surface density and lowering the temperature of the film. To this end, two methods for local compression have been used. The first one, that relies on the application of a high magnetic field, is able to attain large quantum parameter values, $\sigma\Lambda^2 \simeq 9$.[8,12] However, to measure the main properties of the quasi-two-dimensional gas becomes difficult due to the large magnetic field.[21] An alternative to this method is to work with thermal compression, in which a small spot on the sample cell is cooled down to a temperature below the one of the cell.[22,23] This second method achieves lower values for quantum degeneracy $\sigma\Lambda^2 \simeq 1.5$ but allows for direct observation of the sample. Up to now, it has not been possible to arrive to the value $\sigma\Lambda^2 \simeq 4$ where the Berezinskii-Kosterlitz-Thouless (BKT) superfluid transition is expected

to set in. Nevertheless, the quantum degeneracy of the gas was observed as a decrease of the three-body recombination rate at temperatures $T = 120$-200 mK and densities $\sigma \simeq 4 \times 10^{12}$ cm^{-2}.[21]

The zero-temperature equations of state of bulk gas[24] H↓ and liquid[25] T↓ were recently calculated using accurate quantum Monte Carlo methods. Properties like the condensate fraction, distribution functions, and localization of the gas(liquid)-solid phase transitions were established with the help of the *ab initio* H↓-H↓ interatomic potential.[9,26,27] From the theoretical side, much less is known about the ground-state properties of two-dimensional H↓ or H↓ adsorbed on a free ^{4}He surface. In a pioneering work, Mantz and Edwards[18] used the variational Feynman-Lekner approximation to calculate the effective potential felt by a hydrogen atom on the ^{4}He surface. Solving the Schrödinger equation for the atom in this effective potential they concluded that H↓, D↓, and T↓ have a single bound state and calculated the respective binding energies. The main drawback of this treatment is that the adsorbent is substituted by an effective field representing a static and undisturbed surface. In fact, a quantitatively accurate approach to this problem requires a good model for the ^{4}He surface.[19] The use of accurate He-He potentials and ground-state quantum Monte Carlo methods proved to be able to reproduce experimental data directly related to the surface, like the surface tension and the surface width.[28] In the present work, we rely on a similar methodology to the one previously used in the study of the free ^{4}He surface[28] in order to microscopically characterize the ground-state of H↓ adsorbed on its surface. Our study is complemented by a purely two-dimensional simulation of H↓ in order to establish the degree of two-dimensionality of the adsorbed film.

The rest of the paper is organized as follows. The quantum Monte Carlo method used for this study is described in Sec. II. The results obtained for H↓ adsorbed on the ^{4}He surface within a slab geometry are presented in Sec. III together with the comparison with the strictly two-dimensional case. Finally, Sec. IV comprises a brief summary and the main conclusions of the work.

II. QUANTUM MONTE CARLO METHOD

We have studied the ground-state (zero temperature) properties of a thin layer of H↓ adsorbed on the free surface of a ^{4}He slab and also the limiting case of a strictly two-dimensional H↓ gas. Focusing first on the slab geometry, the Hamiltonian of the system composed by $N_{\rm He}$ ^{4}He and $N_{\rm H}$ H↓ atoms is

$$H = -\frac{\hbar^2}{2m_{\rm He}}\sum_{I=1}^{N_{\rm He}}\nabla_I^2 - \frac{\hbar^2}{2m_{\rm H}}\sum_{i=1}^{N_{\rm H}}\nabla_i^2 + \sum_{1=I<J}^{N_{\rm He}} V_{\rm He-He}(r_{IJ}) + \sum_{1=i<j}^{N_{\rm H}} V_{\rm H-H}(r_{ij}) + \sum_{1=I,i}^{N_{\rm He},N_{\rm H}} V_{\rm He-H}(r_{Ii}), \quad (2)$$

with capital and normal indices standing for ^{4}He and H↓ atoms, respectively. It is worth noticing that Freed[29] proved that spin-polarized hydrogen atoms behave as effective bosons within the Born-Oppenheimer approximation. According to Freed's argument, since all electron spins are down, the orbital part of the many-electron wave function in the field of the "clamped nuclei" is antisymmetric with respect to electron permutations. But it is also antisymmetric with respect to nuclear coordinates. Thus, it immediately follows that the many-particle wave function of all the protons in the effective-potential of the electrons has to be symmetric with respect to permutations of the protons. We thus treat H↓ atoms as point-like bosons interacting with a model potential.

The pair potential between He atoms is the Aziz HFD-B(HE) model,[30] used extensively in microscopic studies of liquid and solid helium. The H↓-H↓ interaction ($b^3\Sigma_u^+$ triplet potential) was calculated with high accuracy by Kolos and Wolniewicz (KW).[9] More recently, this potential was recalculated up to larger interatomic distances by Jamieson, Dalgarno, and Wolniewicz (JDW).[26] We have used the JDW data smoothly connected with the long-range behavior of the H↓-H↓ potential as calculated by Yan *et al.*[27] The JDW potential has a core diameter of 3.67 Å and a minimum $\epsilon = -6.49$ K (slightly deeper than KW) at a distance $r_{\rm m} = 4.14$ Å. Finally, we take the H-He pair potential from Das *et al.*;[31] this model was used in the past in the study of a single H↓ impurity[16] in liquid ^{4}He and in mixed T↓-^{4}He clusters.[32] The Das potential[31] has a minimum $\epsilon = -6.53$ K at a distance $r_{\rm m} = 3.60$ Å.

The quantum N-body problem is solved stochastically using the diffusion Monte Carlo (DMC) method.[33] DMC is nowadays one of the most accurate tools for the study of quantum fluids and gases, providing exact results for boson systems within some statistical errors. In brief, DMC solves the imaginary-time (τ) N-body Schrödinger equation for the function $f(\boldsymbol{R},\tau) = \psi(\boldsymbol{R})\Psi(\boldsymbol{R},\tau)$, with $\Psi_0(\boldsymbol{R}) = \lim_{\tau\to\infty}\Psi(\boldsymbol{R},\tau)$ the exact ground-state wave function. The auxiliary wave function $\psi(\boldsymbol{R})$ acts as a guiding wave function in the diffusion process towards the ground state when $\tau \to \infty$. The direct statistical sampling with $f(\boldsymbol{R},\tau)$, called mixed estimator, is unbiased for the energy but not completely for operators which do not commute with the Hamiltonian. In these cases, we rely on the use of pure estimators based on the forward walking strategy.[34] The influence of the finite time step used in the iterative process is reduced by working with a second-order expansion for the imaginary-time Green's function.[35] The last systematic error that one has to deal with is the finite number of walkers $\boldsymbol{R}_i$ which represent the wave function $\Psi(\boldsymbol{R},\tau)$. As usual, we analyze which is the number of walkers required to reduce any bias coming from it to the level of the statistical uncertainties.

The ^{4}He surface is simulated using a slab which grows symmetrically in the z direction and with periodic boundary conditions in the x–y plane.[28] The guiding wave function is then the product of two terms:

$$\psi(\boldsymbol{R}) = \psi_J(\boldsymbol{R})\,\phi(\boldsymbol{R}), \quad (3)$$

the first one accounting for the dynamical correlations induced by the interatomic potentials and the second for the finite size of the liquid in the z direction. Explicitly, $\psi_J(\boldsymbol{R})$ is built as a product of two-body Jastrow factors between the

different particles:

$$\psi_J(\boldsymbol{R}) = \prod_{1=I<J}^{N_{\rm He}} f_{\rm He}(r_{IJ}) \prod_{1=i<j}^{N_{\rm H}} f_{\rm H}(r_{ij}) \prod_{1=I,i}^{N_{\rm He},N_{\rm H}} f_{\rm He-H}(r_{Ii}) \,. \tag{4}$$

The one-body correlations that confine the system to a slab geometry are introduced in $\phi(\boldsymbol{R})$:

$$\phi(\boldsymbol{R}) = \prod_{I=1}^{N_{\rm He}} h_{\rm He}(z_I) \prod_{i=1}^{N_{\rm H}} h_{\rm H}(z_i) \,. \tag{5}$$

The ^{4}He-^{4}He ($f_{\rm He}(r)$) and ^{4}He-H↓ ($f_{\rm He-H}(r)$) two-body correlation factors (4) are chosen of Schiff-Verlet type,

$$f(r) = \exp\left[-\frac{1}{2}\left(\frac{c}{r}\right)^5\right], \tag{6}$$

whereas the H↓-H↓ one is taken as

$$f_{\rm H}(r) = \exp[-b_1 \exp(-b_2 r)], \tag{7}$$

because it was shown to be variationally better for describing the hydrogen correlations.[24] The parameters entering Eqs. (6) and (7) have been optimized using the variational Monte Carlo method. We have used $c_{\rm He} = c_{\rm He\text{-}H} = 3.07$ Å, $b_1 = 101$, and $b_2 = 1.30$ Å^{-1}, neglecting their slight dependence on density. The one-body functions in Eq. (5) are of Fermi type,

$$h(z) = \{1 + \exp[\,k(\,|z - z_{\rm cm}| - z_0)]\}^{-1} \,, \tag{8}$$

with variational parameters k and z_0 related to the width and location of the interface, respectively. The main goal of these one-body terms is to avoid eventual evaporation of particles by introducing a restoring drift force only when particles want to escape to unreasonable distances. Any spurious kinetic energy contribution due to the movement of the center of mass of the full system (^{4}He+H↓) is removed by subtracting $z_{\rm cm}$ from each particle coordinate z, either of ^{4}He or H↓, in Eq. (8). The optimal values used in the DMC simulations are $z_0(^4\text{He})$=22.10 Å, z_0(H↓)=37.06 Å, and $k(^4\text{He})$=k(H↓)=1 Å^{-1}.

Our study of the thin layer of H↓ adsorbed on ^{4}He is complemented with some calculations of a strictly 2D H↓ gas with the Hamiltonian

$$H_{\rm 2D} = -\frac{\hbar^2}{2m_{\rm H}} \sum_{i=1}^{N_{\rm H}} \nabla_i^2 + \sum_{1=i<j}^{N_{\rm H}} V_{\rm H-H}(r_{ij}) \,, \tag{9}$$

using as a guiding wave function a Jastrow factor with the same two-body correlation factors as in the slab (7).[36]

III. RESULTS

The ^{4}He surface where H↓ is adsorbed is simulated with the DMC method using a slab geometry. We use a square cell in the x–y plane that is made continuous by considering periodic boundary conditions in both directions. In the transverse direction z the system is finite, with two symmetric free surfaces at the same distance from the center $z = 0$. The surface of the basic simulation cell is $A = 290.30$ Å^2 and $N_{\rm He} = 324$. With these conditions we guarantee an accurate model for the free surface of ^{4}He, as shown in Ref. 28.

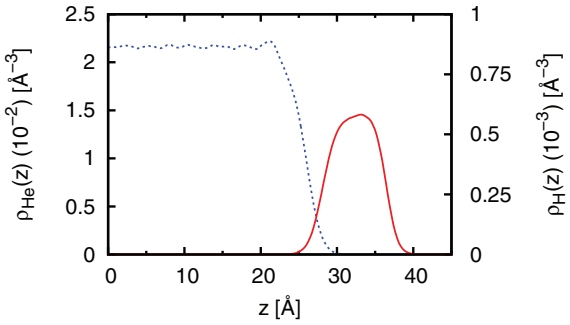

FIG. 1. Density profile of the ^{4}He slab (dashed line) and of the H↓ adsorbed gas (solid line) corresponding to a surface density $\sigma = 9.57 \times 10^{-3}$ Å^{-2}.

On top of one of the slab surfaces we introduce a variable number $N_{\rm H}$ of H↓ atoms that form a thin layer of surface densities $\sigma = N_{\rm H}/A$. In order to reach lower densities than $\sigma = 1/A$ we have replicated the basic slab cell the required number of times. In Fig. 1, we show the density profiles of the ^{4}He slab and of the H↓ layer for a surface density $\sigma = 9.57 \times 10^{-3}$ Å^{-2}. This layer has an approximate width of 8 Å and virtually *floats* on the helium surface: the center of the H↓ layer is located out of the surface, where the ^{4}He density is extremely small. The picture is similar to the one obtained previously by Mantz and Edwards[18] in a variational description of the adsorption of a single H↓ atom. However, contrarily to the exponential tail of the density profile derived by Krotscheck and Zillich[19] in a thorough description of the impurity problem, we observe a faster decay to zero and a rather isotropic profile. We attribute this difference to the residual bias of the one-body factor $h(z)$ (8) used to avoid spurious evaporation of particles. On the other hand, the more well studied case of ^{3}He adsorbed on the ^{4}He surface shows a similar density profile,[37] located on the surface, but in this case centered not so far from the bulk.

One of the most relevant magnitudes that characterize the H↓ film is its energy per particle at different coverages. In Fig. 2, we plot the DMC energy per particle of H↓ as a function of the surface density σ. In order to better visualize the energy of the adsorbed gas, we have subtracted from the computed energies the energy in the infinite dilution limit $\sigma \to 0$.

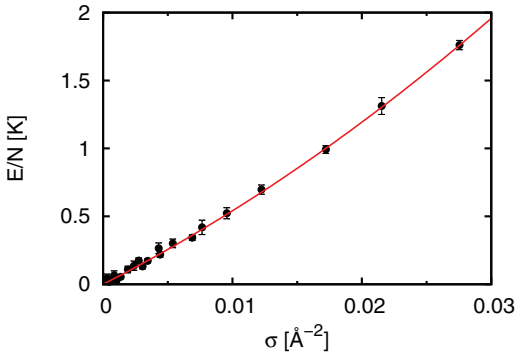

FIG. 2. Energy per particle of H↓ on top of the ^{4}He surface (points with error bars). The energy at the zero-dilution limit is subtracted in such a way that the energy is zero in the limit $\sigma \to 0$. The line on top of the DMC data corresponds to the polynomial fit of Eq. (10).

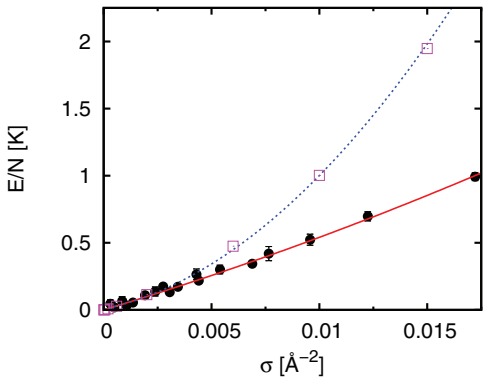

FIG. 3. Comparison between the energy per particle of H↓ adsorbed on the ^{4}He slab (full circles) and the energy of purely two-dimensional H↓ (open squares). The solid line is the polynomial fit (10) and the dotted line is a fit of the 2D energies (11).

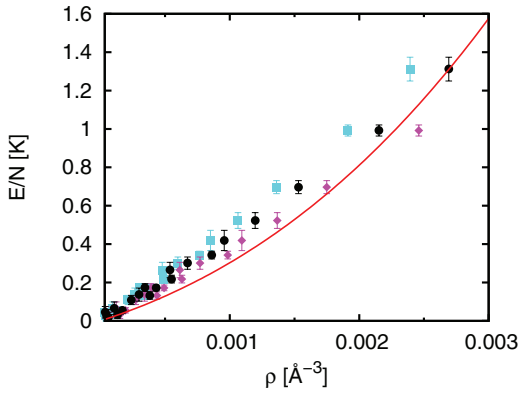

FIG. 4. Comparison between the energy per particle of H↓ adsorbed on the ^{4}He slab and the energy of bulk H↓ (solid line) from Ref. 24. Full squares, full circles, and full diamonds correspond to the layer where we have considered a width in z of 9, 8, and 7 Å, respectively.

The energy increases monotonously with the density and its behavior is well accounted for by the simple polynomial law

$$E/N(\sigma) = B\sigma + C\sigma^2 , \tag{10}$$

with optimal parameters $B = 48(2)$ KÅ^2 and $C = 5.6(9) \times 10^2$ KÅ^4, the figures in parenthesis being the statistical uncertainties.

H↓ floating on top of the ^{4}He free surface has been currently considered as a nice representation of a quasi-two-dimensional quantum gas. In order to be quantitatively accurate in this comparison, we have carried out DMC simulations of strictly 2D H↓ gas without any adsorbing surface.[36] The results obtained for the energy per particle of the 2D gas at different densities are shown in Fig. 3. The energies are well reproduced by a polynomial law

$$E/N(\sigma) = B_{2D}\sigma + C_{2D}\sigma^2 , \tag{11}$$

with $B_{2D} = 35(3)$ KÅ^2 and $C_{2D} = 6.4(1) \times 10^4$ KÅ^4. In the same figure, we plot the energies for the adsorbed gas at the same coverage. As one can see, the agreement between the strictly 2D gas and the film is good for densities $\sigma \lesssim 5 \times 10^{-3}$ Å^{-2}. At higher densities, the additional degree of freedom in the z direction makes the growth of the energy with the surface density in the layer nearly linear up to the shown density, in contrast with the significant quadratic increase observed in the 2D gas ($C \ll C_{2D}$). The difference between energies of the layer and the 2D gas thus increases with the surface density, which correlates with the increase of the layer width from approximately 7 to 9 Å.

A possible scenario when the density increases and the equation of state of the layer departs from the 2D law is the existence of a nearly three-dimensional gas. We have analyzed this possibility by considering a width in z given by the density profile (Fig. 1) and by estimating the 3D density of the adsorbed gas as the coverage divided by the layer width. In Fig. 4, we show the energy per particle of adsorbed H↓ as a function of the density considering our best estimation for the layer width, $z = 8$ Å, and also $z = 9$ and 7 Å. The possible 3D behavior of the energy is analyzed by comparing the results of the layer with the ones of the bulk 3D gas. At low densities, the energies of the adsorbed phase are higher than the 3D gas and, when the density increases, both results tend to cross. As one can see, the energies of adsorbed H↓ are not well described by a 3D equation of state at any density within the regime studied.

The structure and the distribution functions of H↓ atoms in the layer can be studied by doing slices of small width ($\Delta z = 1$ Å) and, within a given slice, as a function of the radial distance between particles in the plane $r = \sqrt{x^2 + y^2}$. In Fig. 5, we report results of the two-body radial distribution function $g(z, r)$ where z is the distance to the center of the ^{4}He slab at a coverage $\sigma = 0.0215$ Å^{-2}. Around the center of the H↓ density profile, $g(r)$ is nearly independent of z with a main peak of a height smaller than 1.2. In the wings of $\rho_H(z)$, where the local density is smaller, $g(r)$ shows less structure and the noise of the DMC data also increases due to low statistics.

It is interesting to know if the spatial structure of H↓ atoms on the ^{4}He surface is similar to the one in a strictly 2D geometry. To this end, we show in Fig. 6 results of the radial distribution function for both systems at the same surface density ($\sigma = 0.0095$ Å^{-2}). The result corresponding to the layer is taken from a slice Δz in the center of the density profile. As one can see, both functions do not show any significant peak because the density is rather small. However, the behavior at small interparticle distances is appreciably different. In the layer, atoms can be closer (in the in-plane

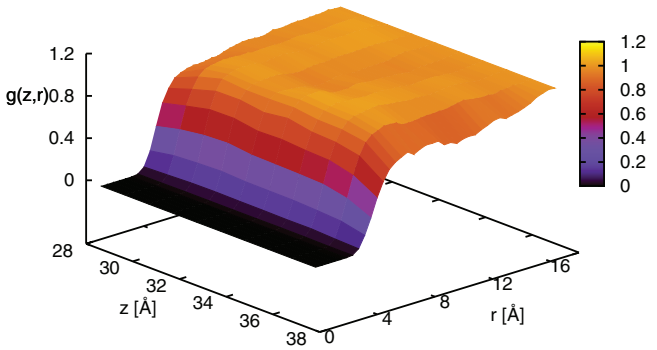

FIG. 5. Two-body distribution function $g(z, r)$ of H↓ adsorbed on ^{4}He, with $r = \sqrt{x^2 + y^2}$, at surface density $\sigma = 0.0215$ Å^{-2}.

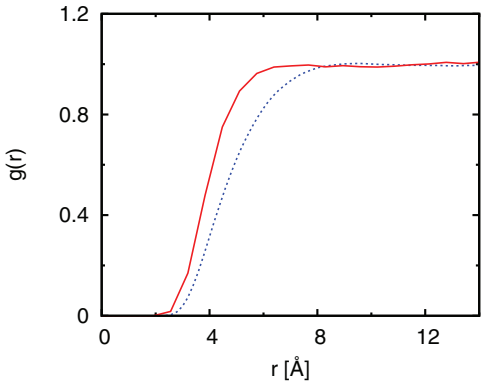

FIG. 6. Comparison between the two-body distribution function in the center of the slab, corresponding to the density $\sigma = 0.0095$ Å^{-2} (solid line) with the one corresponding to a purely 2D H↓ gas at the same surface density (dotted line).

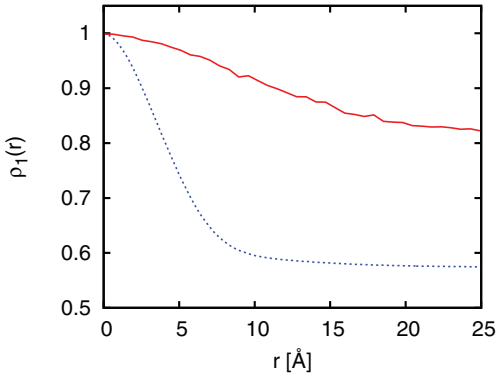

FIG. 8. Comparison between the one-body distribution function in the center of the slab, corresponding to a density $\sigma = 0.0095$ Å^{-2} (solid line) with the one corresponding to a purely 2D H↓ gas at the same surface density (dotted line).

distance $r = \sqrt{x^2 + y^2}$) than in 2D because of the small but nonzero width of the slice used for its calculation. In fact, we have shown previously in Fig. 2 that, at the density $\sigma = 0.0095$ Å^{-2} used in Fig. 6, the energies per particle of the layer and the strictly 2D gas start to be significantly different, in agreement with the differences observed here in the distribution function $g(r)$.

A key magnitude in the study of any quantum Bose gas is the one-body distribution function $\rho_1(r)$ since it furnishes evidence of the presence of off-diagonal long-range order in the system. As it is well known, its asymptotic behavior in a homogeneous system $\lim_{r\to\infty}\rho_1(r) = n_0$ gives the fraction of particles occupying the zero-momentum state, that is the condensate fraction n_0. In Fig. 7, we show a surface plot containing results of $\rho_1(z, r)$ at density $\sigma = 0.0215$ Å^{-2}, obtained following the same method as in the grid of $g(z, r)$ shown in Fig. 5. In the outer part of the density profile the condensate fraction increases because the density is smaller. When z decreases the condensate fraction also decreases and reaches a plateau in the central part of $\rho_H(r)$. If z is reduced even more and $\rho_{He}(r)$ starts to increase, the H↓ condensate fraction decreases again due to the small but nonzero ^{4}He density; the low statistics in this part makes the signal very noisy and therefore we do not plot data for $z < 27$ Å in Fig. 7.

A relevant issue in the study of the off-diagonal long-range order in the adsorbed gas is the *dimensionality* of the results achieved. As we have made before for the two-body distribution functions, we compare $\rho_1(r)$ for a 2D gas and for a slice in the center of the adsorbed layer at the same density in Fig. 8. The results show that in this case the behavior in the layer is significantly different from the one observed in strictly 2D. The difference is larger than the one we have observed at the same density for $g(r)$ (Fig. 6), with values for the condensate fraction that differ in ∼30%. The condensate fraction of the 2D gas is clearly smaller than the one of the layer due to the transverse degree of freedom z that translates into an effective surface density smaller than the one of the full layer.

The density dependence of the condensate fraction of adsorbed H↓ is shown in Fig. 9. The values reported have been obtained from the asymptotic value of the one-body distribution function in the central part of the density profile. As expected, the condensate fraction is nearly 1 at very low densities and then decreases when σ increases. However, the decrease is quite slow in such a way that even at densities as large as $\sigma = 0.02$ Å^{-2} the condensate fraction is still $n_0 \simeq 0.6$. At the same density, the condensate fraction of the 2D gas is half this value, $n_0 \simeq 0.3$. The dependence of n_0 with the density for the 2D geometry, shown in Fig. 9 for

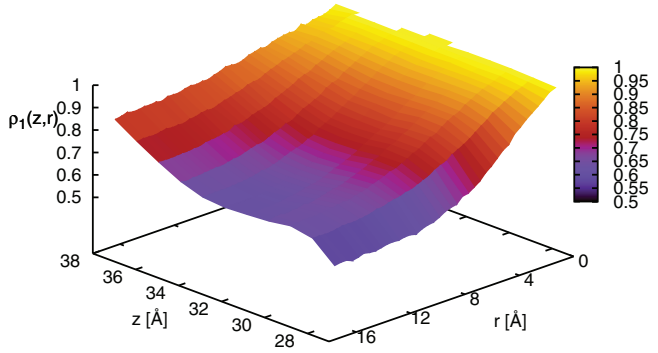

FIG. 7. One-body distribution function $\rho_1(z, r)$ of H↓ adsorbed on ^{4}He, with $r = \sqrt{x^2 + y^2}$, at surface density $\sigma = 0.0215$ Å^{-2}.

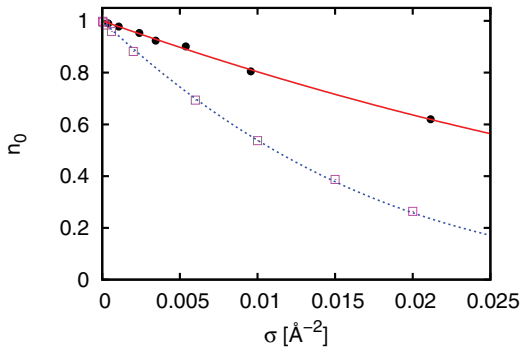

FIG. 9. Condensate fraction as a function of the surface density σ. Solid circles correspond to H↓ on ^{4}He and open squares to a 2D gas. The lines on top of the DMC data are fits to guide the eye.

comparison, is significantly stronger with a larger depletion of the condensate fraction for all densities.

IV. SUMMARY AND CONCLUSIONS

The experimental realization of an extremely thin layer of H↓ adsorbed on the surface of superfluid ^{4}He provides a unique opportunity for the study of nearly two-dimensional quantum gases. The system is stable and the influence of the liquid substrate is nearly negligible, without the corrugation effects that a solid surface like graphite provides. Moreover, spin-polarized hydrogen is a specially appealing system from the theoretical side because it is the best example of quantum matter (it remains gas even in the zero temperature limit) and its interatomic interaction is known with high accuracy. In the present work, we have addressed its study from a microscopic approach relying on the use of quantum Monte Carlo methods by means of a simulation that incorporates the full Hamiltonian of the system, composed of a realistic ^{4}He surface and the layer of H↓ adsorbed on it.

From very low coverages up to relatively high surface densities, we have reported results of the main properties of adsorbed H↓: energy, density profile, two- and one-body distribution functions, and the condensate fraction. Our results point to an ∼8 Å thick layer that virtually *floats* on top of ^{4}He. We have calculated the energy as a function of the surface density σ and compared these energies with the results obtained in a purely 2D H↓ gas in order to establish the degree of two-dimensionality of the layer. The agreement between both simulations is only satisfactory for small densities $\sigma \lesssim 5 \times 10^{-3}$ Å^{-2} and, from then on, the additional degree of freedom in the z direction of the layer causes its energy to grow slower than in strictly 2D. Significant departures of strictly 2D behavior are also observed in the two-body radial distribution function and mainly in the condensate fraction values. Our DMC results show that the condensate fraction for the layer is appreciably higher than in 2D, with values as large as $n_0 = 0.6$ at the largest coverages studied. If we convert this coverage to volume density by using the layer width of 8 Å, we see that the condensate fraction is quite close to published 3D values in Ref. 24. From these results we can be certain that a BKT phase transition would be a realistic scenario at low surface densities. For higher densities, further study using intensive path-integral Monte Carlo simulations at finite temperatures would be needed.

ACKNOWLEDGMENTS

J.B. acknowledges partial financial support from the DGI (Spain) Grant No. FIS2011-25275, Generalitat de Catalunya Grant No. 2009SGR-1003, and Qatar National Research Fund NPRP 5-674-1-114s. L.V.M. acknowledges support from MSES (Croatia) under Grant No. 177-1770508-0493.

[1] W. C. Stwalley and L. H. Nosanow, Phys. Rev. Lett. **36**, 910 (1976).
[2] M. D. Miller and L. H. Nosanow, Phys. Rev. B **15**, 4376 (1977).
[3] I. F. Silvera, and J. T. M. Walraven, in *Progress in Low Temperature Physics*, edited by D. F. Brewer (Elsevier, Amsterdam, 1986), Vol. X, p. 139.
[4] T. J. Greytak, in *Bose-Einstein Condensation*, edited by A. Griffin, D. W. Snoke, and S. Stringari (Cambridge University Press, Cambridge, 1995), p. 131.
[5] I. F. Silvera, in *Bose-Einstein Condensation*, edited by A. Griffin, D. W. Snole, and S. Stringari (Cambridge University Press, Cambridge, 1995), p. 160.
[6] D. G. Fried, T. C. Killian, L. Willmann, D. Landhuis, S. C. Moss, P. Kleppner, and T. J. Greytak, Phys. Rev. Lett. **81**, 3811 (1998).
[7] M. H. Anderson, J. R. Ensher, M. R. Matthews, C. E. Wieman, and E. A. Cornell, Science **269**, 198 (1995); K. B. Davis, M. O. Mewes, M. R. Andrews, N. J. van Druten, D. S. Durfee, D. M. Kurn, and W. Ketterle, Phys. Rev. Lett. **75**, 3969 (1995); C. C. Bradley, C. A. Sackett, J. J. Tollet, and R. G. Hulet, *ibid.* **75**, 1687 (1995).
[8] A. I. Safonov, S. A. Vasilyev, I. S. Yasnikov, I. I. Lukashevich, and S. Jaakkola, Phys. Rev. Lett. **81**, 4545 (1998).
[9] W. Kolos and L. Wolniewicz, J. Chem. Phys. **43**, 2429 (1965); Chem. Phys. Lett. **24**, 457 (1974).
[10] J. T. M. Walraven, in *Fundamental Systems in Quantum Optics*, edited by J. Dalibard, J. M. Raimond, and J. Zinn-Justin (Elsevier, Amsterdam, 1992), p. 487.
[11] J. J. Berkhout and J. T. M. Walraven, Phys. Rev. B **47**, 8886 (1993).
[12] A. P. Mosk, M. W. Reynolds, T. W. Hijmans, and J. T. M. Walraven, Phys. Rev. Lett. **81**, 4440 (1998).
[13] J. Järvinen, J. Ahokas, and S. Vasiliev, J. Low Temp. Phys. **147**, 579 (2007).
[14] J. Ahokas, J. Järvinen, and S. Vasiliev, Phys. Rev. Lett. **98**, 043004 (2007).
[15] J. Järvinen and S. Vasilyev, J. Phys.: Conf. Ser. **19**, 186 (2005).
[16] J. M. Marín, J. Boronat, and J. Casulleras, J. Low Temp. Phys. **110**, 205 (1998).
[17] A. I. Safonov, S. A. Vasilyev, A. A. Kharitonov, S. T. Boldarev, I. I. Lukashevich, and S. Jaakkola, Phys. Rev. Lett. **86**, 3356 (2001).
[18] I. B. Mantz and D. O. Edwards, Phys. Rev. B **20**, 4518 (1979).
[19] E. Krotscheck and R. E. Zillich, Phys. Rev. B **77**, 094507 (2008).
[20] I. F. Silvera and V. V. Goldman, Phys. Rev. Lett. **45**, 915 (1980).
[21] J. Järvinen, J. Ahokas, S. Jaakkola, and S. Vasilyev, Phys. Rev. A **72**, 052713 (2005).
[22] A. Matsubara, T. Arai, S. Hotta, J. S. Korhonen, T. Suzuki, A. Masaike, J. T. M. Walraven, T. Mizusaki, and A. Hirai, Physica B **194–196**, 899 (1994).
[23] S. Vasilyev, J. Järvinen, A. Safonov, and S. Jaakkola, Phys. Rev. A **69**, 023610 (2004).
[24] L. Vranješ Markić, J. Boronat, and J. Casulleras, Phys. Rev. B **75**, 064506 (2007).
[25] I. Bešlić, L. Vranješ Markić, and J. Boronat, Phys. Rev. B **80**, 134506 (2009).
[26] M. J. Jamieson, A. Dalgarno, and L. Wolniewicz, Phys. Rev. A **61**, 042705 (2000).
[27] Z.-C. Yan, J. F. Babb, A. Dalgarno, and G. W. F. Drake, Phys. Rev. A **54**, 2824 (1996).
[28] J. M. Marín, J. Boronat, and J. Casulleras, Phys. Rev. B **71**, 144518 (2005).
[29] J. H. Freed, J. Chem. Phys. **72**, 1414 (1980).
[30] R. A. Aziz, F. R. W. McCourt, and C. C. K. Wong, Mol. Phys. **61**, 1487 (1987).
[31] G. Das, A. F. Wagner, and A. C. Wahl, J. Chem. Phys. **68**, 4917 (1978).
[32] P. Stipanović, L. Vranješ Markić, J. Boronat, and B. Kežić, J. Chem. Phys. **134**, 054509 (2011).
[33] B. L. Hammond, W. A. Lester, Jr., and P. J. Reynolds, *Monte Carlo Methods in ab initio Quantum Chemistry* (World Scientific, Singapore, 1994).
[34] J. Casulleras and J. Boronat, Phys. Rev. B **52**, 3654 (1995).
[35] J. Boronat and J. Casulleras, Phys. Rev. B **49**, 8920 (1994).
[36] A study of the phase diagram of strictly two-dimensional H↓gas can be found in L. Vranješ Markić and J. Boronat, J. Low. Temp. Phys. **171**, 685 (2013).
[37] R. Guardiola and J. Navarro, Phys. Rev. Lett. **89**, 193401 (2002).